

# Shifts in carbon partitioning by photosynthetic activity increase terpenoid synthesis in glandular trichomes

Nima P. Saadat<sup>1,3\*</sup> | Marvin van Aalst<sup>1\*</sup> | Alejandro Brand<sup>2</sup> | Oliver Ebenhöf<sup>1,3</sup> | Alain Tissier<sup>2</sup> | Anna B. Matuszyńska<sup>3,4</sup>

<sup>1</sup>Institute of Theoretical and Quantitative Biology, Heinrich Heine University Düsseldorf, 40225 Düsseldorf, Germany

<sup>2</sup>Leibniz-Institut für Pflanzenbiochemie, Weinberg 3, 06120 Halle, Germany

<sup>3</sup>Cluster of Excellence on Plant Sciences, Heinrich Heine University Düsseldorf, Universitätsstraße 1, 40225 Düsseldorf, Germany

<sup>4</sup>Computational Life Science, Department of Biology, RWTH Aachen University, Worringerweg 1, 52074 Aachen, Germany

## Correspondence

Email: nima.saadat@hhu.de;

marvin.van.aalst@hhu.de;

anna.matuszynska@rwth-aachen.de

## Funding information

This work was funded by the Deutsche Forschungsgemeinschaft Research Grant - project ID 420069095 (AB, AT, AM), Deutsche Forschungsgemeinschaft under Germany's Excellence Strategy - EXC-2048/1 - project ID 390686111 (NS, OE, AM), and EU's Horizon 2020 research and innovation programme under the Grant Agreement 862087 (MvA).

**Abbreviations:** CBB, Calvin-Benson-Bassham cycle; DMAPP, dimethylallyl diphosphate; FBA, flux-balance analysis; F6P, Fructose-6-Phosphate; GEM, genome-scale metabolic models; GT, glandular trichome; IPP, isopentenyl diphosphate; LP, linear programming; MEP, methyl-erythritolphosphate pathway; MEV, mevalonate pathway; PEPC, Phosphoenolpyruvate carboxylase; PETC, photosynthetic electron transfer chain; TCA, tricarboxylic acid

\*Equally contributing authors.

Several commercially important secondary metabolites are produced and accumulated in high amounts by glandular trichomes, giving the prospect of using them as metabolic cell factories. Due to extremely high metabolic fluxes through glandular trichomes, previous research focused on how such flows are achieved. The question regarding their bioenergetics became even more interesting with the discovery of photosynthetic activity in some glandular trichomes. Despite recent advances, how primary metabolism contributes to the high metabolic fluxes in glandular trichomes is still not fully elucidated. Using computational methods and available multi-omics data, we first developed a quantitative framework to investigate the possible role of photosynthetic energy supply in terpenoid production and next tested experimentally the simulation-driven hypothesis. With this work, we provide the first reconstruction of specialised metabolism in Type-VI photosynthetic glandular trichomes of *Solanum*

*lycopersicum*. Our model predicted that increasing light intensities results in a shift of carbon partitioning from catabolic to anabolic reactions driven by the energy availability of the cell. Moreover, we show the benefit of shifting between isoprenoid pathways under different light regimes, leading to a production of different classes of terpenes. Our computational predictions were confirmed *in vivo*, demonstrating a significant increase in production of monoterpenoids while the sesquiterpenes remained unchanged under higher light intensities. The outcomes of this research provide quantitative measures to assess the beneficial role of chloroplast in glandular trichomes for enhanced production of secondary metabolites and can guide the design of new experiments that aim at modulating terpene production.

#### KEYWORDS

bioenergetics, glandular trichomes, photosynthesis, stoichiometric model, secondary metabolites, terpenes

## 1 | INTRODUCTION

Most plant species exhibit cellular outgrowths of their epidermis called trichomes. Due to their often species-specific characteristic, many criteria for classification exist, the most popular one being the division into non-glandular and **glandular trichomes** (GT) [1]. Whilst non-glandular trichomes serve more as a physical and mechanical defence against biotic and abiotic stresses, all GTs are characterised by the ability to synthesise and accumulate vast amounts of valuable specialised (secondary) metabolites. Due to extremely high metabolic fluxes in these organs, production of some metabolites can reach up to 20% of the leaf dry weight [2], GTs are often referred to as true **metabolic cell factories** [3]. Products of GTs include terpenoids, phenylpropanoids, flavonoids, fatty acid derivatives, and acyl sugars [4] exhibiting antifungal, insecticide, or pesticide properties. Thereby GTs are not only incredibly important to plant fitness, as they contribute to the chemical arsenal of plants, but are also of relevance to multiple industries.

The key carbon source in most GTs of tomatoes is sucrose which is converted into a multitude of organism-specific metabolites in the glands [5]. The massive productivity of hydrocarbon compounds implies, however, a supply of adequate amounts of not only carbon, energy, and reducing power, but also precursors, produced by intermediate pathways. Terpenoids represent the largest and structurally most diverse class of plant metabolites and are major products of GT biosynthesis. Despite their multiplicity, with over 30 000 well-known structures, they are all assemblies of C<sub>5</sub> isoprene units built from isopentenyl diphosphate (IPP) and its isomer dimethylallyl diphosphate (DMAPP). There are two identified pathways for IPP and DMAPP production: i) the plastidial 2-C-methyl-D-erythritol 4-phosphate (MEP) pathway from pyruvate and glyceraldehyde-3-phosphate or ii) the cytosolic mevalonate (MVA) pathway from acetyl-CoA [6]. Although these pathways are thought to be largely independent, some exchange of precursors may occur [7], and such cross-talk requires further investigation. For instance, is there some cross-talk of plastidial and cytosolic

21 pathways providing the 5-carbon precursors, as suggested in the latest work in peppermint [8]? And if so, what effect  
22 does it have on overall productivity? Beyond this, a major issue is the source of energy and its distribution to under-  
23 stand how GTs achieve their high productivity. The question becomes more intriguing when one realises that some of  
24 the GTs contain photosynthetically active chloroplasts (as the type VI GT in *S. lycopersicum* [9]). Considering that in the  
25 case of many plants where the seeds are green during embryogenesis, the light can influence the fatty acid synthesis,  
26 and potentially power refixation of CO<sub>2</sub> [10, 11], we took the challenge to understand whether a similar **effect of light**  
27 can be predicted in trichomes. Till now it is still unclear what the advantages and disadvantages of photosynthetic  
28 GTs are in contrast to non-photosynthetic GTs. Moreover, there is limited research on GTs ability to absorb light. Even  
29 research focused on light intensity-mediated trichome production does not focus on their photosynthetic activity [12].  
30 The separation of cytosolic and chloroplast-bound pathways, as well as the utility of photosynthesis, are until now  
31 only vaguely understood, and the most recent summary of current advances has been recently provided [13].

32 To shed light on the advantages of photosynthetic GT for terpenoid synthesis and secondary metabolism, in-  
33 vestigations of the system's bioenergetics and reaction flux distributions are needed. Mathematical, computational  
34 models provide a coherent framework to study metabolism. Constraint-based stoichiometric models [14] are partic-  
35 ularly adequate for exploratory studies of the systemic properties of a metabolic network and investigations of the  
36 flux distributions. Such models are static and represent mathematically the network of biochemical reactions of an  
37 organism in the form of a matrix [15]. They can focus on various scales, with genome-scale metabolic models (GEMs)  
38 aiming at representing the whole biochemical network of an individual organism. GEMs are constructed by assigning  
39 biochemical functions to enzymes encoded in the genome, and due to the expansion of the whole genome sequencing,  
40 many plant GEMs are currently available, with *Oryza sativa indica* [16], *Arabidopsis thaliana* [17] and *Solanum lycoper-*  
41 *sicum* L. [18] among many others. Flux Balance Analysis (FBA) [19, 20], a mathematical method that allows calculating  
42 the flow of metabolites through the network, is a popular tool to predict the production rate of the compound of in-  
43 terest. FBA requires two assumptions: i) the experimental system is at a steady state, and ii) the network is optimised  
44 to maximise or minimise certain biological outcomes, for instance, its biomass. The so-called, cell-specific, objective  
45 functions in GEMs are optimised in a linear programming approach in which all reaction fluxes are constrained within  
46 given boundaries. This constraint-based analysis of GEMs allows the calculation of optimal flux solutions in different  
47 conditions, therefore allowing investigations on the metabolic fluxes and bioenergetics of systems.

48 In this work, we have reconstructed the metabolism in the photosynthetic glandular trichome type VI of a *Solanum*  
49 *lycopersicum* LA4024 using previously published transcriptome and metabolome data [5]. With a general, mathemat-  
50 ical framework, we investigated the effect of having photosynthetically active machinery inside of a trichome and  
51 systematically tested the model on how GTs achieve high metabolic productivity proposed by Balcke *et al.* [5]. In our  
52 simulations, we observed the increase in terpenoid production under increasing light intensities. Increased photosyn-  
53 thetic activity shifts the partitioning of uptaken carbons from catabolism to anabolism due to increased energy levels.  
54 Bioenergetics and energy levels determine which of the known terpenoid precursor production pathways (MEV, MEP)  
55 is more desirable/optimal in different light/stress conditions. Our model can explain the benefits of having chloroplasts  
56 in GTs and serves as a groundwork for further investigations of the possible cross-talks between the two pathways  
57 of terpenoid precursor synthesis. It complements the previous work by Balcke *et al.* [5] by not only confirming their  
58 hypothesis that the light-dependent reactions of photosynthesis support the secondary metabolite pathways, but  
59 explaining how this support is achieved. Finally, our predictions have been tested *in vivo* and we provide an experi-  
60 mental validation by showing that under high light conditions, production of the most abundant MEP-derived terpenes  
61 (2-carene and  $\beta$ -phellandrene/D-limonene) increases, whilst most abundant MEV-derived terpenes ( $\beta$ -caryophyllene  
62 and  $\alpha$ -humulene) remain unchanged.

## 2 | METHODS

### 2.1 | Choice of the model organism

In this study, we have chosen to investigate type VI GT in the tomato genus. The tomato genus displays seven types of trichomes: II, III and V (non-glandular) and I, IV, VI and VII (glandular trichomes), with type VI being the most abundant one in the *Solanum lycopersicum* species. *S. lycopersicum* serves as an excellent model organism for glandular trichome study due to the availability of i) high-quality complete genome sequence [21], ii) excellent genetic resources [22], iii) comparative multi-omics data [5], iv) several mathematical models available, including whole genome metabolic network reconstruction [18], and v) in contrast to other well-studied organisms like peppermint [23, 24], possession of photosynthetic GT.

### 2.2 | Modelling environment

Our model is implemented in Python, using our in-house developed package `moped`, "an integrative hub for reproducible construction, modification, curation and analysis of metabolic models" [25]. With `moped` all decision processes and modelling steps are well documented in a transparent and repeatable fashion. All details and information about the exact construction process of the model, as well as all investigations and analyses, can be found in our provided scripts at <https://gitlab.com/qtb-hhu/models/glandular-trichomes>. The summary of the construction steps is provided in the section below.

### 2.3 | Model construction and assumptions

Although a genome-scale model of tomato metabolism is available (iHY3410 model [18]), we decided to use a bottom-up approach and perform the reconstruction ourselves, because we were not able to reconstruct the steps of manual curation performed by the authors. We based the model reconstruction on available transcriptomics and metabolomics data [5], the LycoCyc database (tomato metabolic pathway database, version 3.3 [26], available from Solanaceae Genomics Network, <http://www.sgn.cornell.edu>) and biochemical knowledge in plants from scientific publications. All reactions and metabolites found in transcriptomics and metabolomics data have been added to the model from the LycoCyc database using the `moped` metabolic modelling package, ensuring GPR rules for all added reactions in the network.

We used Meneco, a tool for metabolic network completion [27] to subsequently fill gaps in our network with annotated reactions from the LycoCyc database, so our model is capable of synthesizing all compounds found within the metabolomics data [5], all terpenoids found in photosynthetic GTs of tomato [28] as well as all amino acids, nucleotide bases and lipid precursors from sucrose, light, orthophosphate, ammonia, sulfate, protons and water. All reactions in our model have been checked for mass and charge balance and are able to carry steady-state fluxes. Our model shows the ability to synthesize biomass precursors and terpenoids on a realistic scale. The model has been examined for inconsistencies in energy metabolism by analyzing the model behaviour according to changes in ATP demand. Increasing ATP demand leads to plausible changes in key reactions of the model, such as a decrease in objective function flux. A detailed description of every implemented step in model construction, as well as the code for reproducing the entire model reconstruction process, can be found in our `model_construction.ipynb` notebook in the supplementary material.

Our model is a data-driven, yet simplified, constraint-based model which is ensured not to include infeasible

100 energy and mass-generating cycles. Within our model simplifications, we found that a model consisting of three  
101 essential compartments (cytosol, intermembrane space and extracellular space, as represented on Fig. 1) is able to  
102 represent photosynthetic GT metabolic profiles. While detailed compartmental separation is common practice in  
103 large genome-scale metabolic models, it would not make any difference to the results of our model simulations due  
104 to the fact that there are several intercompartmental transporters between the chloroplast and the cytosol for energy  
105 equivalents like ATP and other key metabolites [29]. Adding over-detailed compartmentalisation to the model would  
106 therefore not alter any of our results and is left out for the sake of model simplicity and preventing unfavourable model  
107 modifications. The resulting model consists of 1307 reactions and 1371 metabolites and thanks to the integration of  
108 the multiomics data, its behaviour has been ensured to match reported experimental observations [5]. There are nine  
109 exchange reactions, allowing the free exchange of inorganic metabolites such as oxygen, as well as light absorption  
110 and sucrose uptake. To ensure the highest quality and consistency our model has been thoroughly inspected using  
111 the MEMOTE standardised testing suite [30].

### 112 2.3.1 | Optimisation and objective function

113 In most constraint-based models and their analyses, the maximization objective is the production of biomass [31].  
114 While this may be applicable for prokaryotic organisms, we doubt that photosynthetic glandular trichome cells are  
115 maximising the increase of their replication rate, and rather maximise terpenoid synthesis while also having a manda-  
116 tory production rate of macromolecules to keep cells intact. For this, our model includes an objective function to  
117 produce terpenoids while requiring a fixed flux through a function of biomass synthesis, consuming typical compo-  
118 nents like amino acids, sugars, nucleotides, cell wall, and fatty acid precursors. We used a simplified biomass function  
119 inspired by plant biomass functions from Seaver *et al.* [32], similar to standard biomass functions used successfully for  
120 FBA in plants [33, 34]. Our aim was to capture the necessity for growth and self-repair, while setting the objective  
121 function to maximize the production of terpenoids. To describe additional energy required for the maintenance of  
122 cells, we implemented a representative reaction for ATP maintenance, as it is common practice in metabolic modelling  
123 [35].

### 124 2.3.2 | Calculation of flux units and light intensity units

125 There is limited research on GTs ability to absorb light (e.g., [36]), and we have not found any dedicated research  
126 focused on the optical properties of GTs. Overall, while there is some evidence to suggest that GTs may have optical  
127 properties allowing for some light absorption, more research is needed to fully understand their ability to absorb light.  
128 Therefore we have decided to estimate the maximal absorption rate based on the reported maximal production fluxes.  
129 Light is therefore represented as **photons absorbed by the photosystems** used for photosynthesis in contrast to the  
130 incident light that will be several-fold higher.

131 Although it is known that due to diel cycles of photosynthesis different metabolic flux patterns in the light and the  
132 dark are observed and require different treatments for the optimisation problem[37], our FBA on the trichome model  
133 is performed under continuous light. The units of light absorption are represented in  $\frac{\mu\text{molPhotons}}{\text{s}\cdot\text{m}^2}$  and the detailed  
134 calculations are provided in the Supporting Information. As it has been reported that carbon dioxide exchange is 100  
135 times lower in photosynthetic GTs than in leaves we decided not to include a carbon dioxide influx, however, carbon  
136 dioxide is produced in the system and can flow out of the model [5].

137 A suggested terpenoid production rate of GTs has been provided by Turner *et al.* [38] at  $0.017 \frac{\text{nmol}}{\text{h}\cdot\text{gland}}$ . Assuming  
138 that this rate can be applied to the maximal terpenoid production rate of photosynthetic GTs of tomatoes, we trans-

139 form our calculated fluxes to the corresponding units by  $\text{Flux} \cdot \frac{0.017 \frac{\text{nmol}}{\text{hgland}}}{\text{max. Terp flux}}$ . Next, in order to convert the fluxes of  
 140 photons into units of light intensities, we calculated the light-absorbing surface of the GT type VI. Although the head  
 141 of GT type VI is made up of 4 secretory cells, we simplify the whole surface of the head as a sphere. Based on the  
 142 measured values of the diameters of GTs from [39] and bright-field microscopic image from [9] we took the estimate  
 143 of  $50 \mu\text{m}$  as the diameter. This number can be substituted with a different value and the light conversion function will  
 144 be adapted. Under these assumptions, the surface area can be estimated as:

$$145 \quad A = 4 * \pi \left( \frac{50 \mu\text{m}}{2} \right)^2 = 8000 \mu\text{m}^2 = 8 \cdot 10^{-9} \text{m}^2$$

146 To calculate the conversion factor for the photon absorption of GTs, we first calculate the units of photons absorbed  
 147 by the gland at saturated light flux and maximal terpenoid production predicted by our model as:

$$148 \quad 0.017 * \frac{\text{Max. Light Flux}}{\text{Max. Terp. Flux}} = 0.017 * \frac{480}{8.85} = 0.92 \frac{\text{nmol/Photons}}{\text{hgland}}$$

149 To convert this unit into  $\frac{\mu\text{mol}}{\text{s} \cdot \text{m}^2}$ , we first calculate the corresponding unit for  $\frac{\text{nmol/Photons}}{\text{hgland}}$  by:

$$150 \quad \frac{1 \text{nmol/Photons}}{\text{hgland}} = \frac{1}{28800} \frac{\text{mol/Photons}}{\text{s} \cdot \text{m}^2} = 56 \frac{\mu\text{mol/Photons}}{\text{s} \cdot \text{m}^2}$$

151 for our maximal Light flux, this corresponds to  $0.92 \cdot 56 \frac{\mu\text{mol/Photons}}{\text{s} \cdot \text{m}^2} = 51.52 \frac{\mu\text{mol/Photons}}{\text{s} \cdot \text{m}^2}$  as the saturating light intensity,  
 152 providing the light flux conversion factor of  $\text{Light Flux} \cdot \frac{51.52 \frac{\mu\text{mol/Photons}}{\text{s} \cdot \text{m}^2}}{\text{sat. Light flux}}$ .

## 153 2.4 | Experimental set-up

154 The high light experiment was conducted using two LED-light panels (Rhenac GreenTech AG, Hennef, Germany) placed  
 155 inside a phytochamber and separated by a black curtain. Tomato (*Solanum lycopersicum* cv Moneymaker) plants were  
 156 germinated on soil under control conditions (CN): 16h light,  $422 \mu \text{mol m}^{-2} \text{s}^{-1}$  at  $25^\circ\text{C}$  and 8h dark at  $20^\circ\text{C}$ , 70%  
 157 humidity day and night. After 22 days of growth, half of the plants were transferred to high light (HL) conditions for  
 158 further 7 days, where light intensity was adjusted to  $1289 \mu \text{mol m}^{-2} \text{s}^{-1}$ . Light spectra were recorded using a Specbos  
 159 1211UV (JETI, Jena, Germany) photometer (Fig. S1). Volatile terpenoids of leaflets of three different developmental  
 160 stages were collected by surface extraction using leaf discs of 1 cm diameter and vortexed for 30 seconds in n-hexane.  
 161 Mono- and sesquiterpenes were detected using a Trace GC Ultra gas chromatograph coupled with an ATAS Optic  
 162 3 injector and an ISQ mass spectrometer (Thermo Scientific) with electron impact ionization. The chromatographic  
 163 separation was performed on a ZB-5ms capillary column ( $30 \text{m} \times 0.32 \text{mm}$ , Phenomenex). The flow rate of helium was  
 164  $1 \text{ml min}^{-1}$ , and the injection temperature rose from  $60$  to  $250^\circ\text{C}$  at  $10^\circ\text{C sec}^{-1}$  during 30 sec. The GC oven temperature  
 165 ramp was  $50^\circ\text{C}$  for 1 min,  $50$ – $150^\circ\text{C}$  at  $7^\circ\text{C min}^{-1}$  and  $150$ – $300^\circ\text{C}$  at  $25^\circ\text{C min}^{-1}$  for 2 min. Mass spectrometry was  
 166 performed at  $70 \text{eV}$  in full scan mode with  $m/z$  from 50 to 450. Data analysis was done with the Xcalibur software  
 167 (Thermo Scientific).

## 168 3 | RESULTS

169 We used our model to perform a general analysis in which we simulate the rate of terpenoid synthesis over sys-  
 170 tematically increasing light intensities via parsimonious Flux Balance Analysis (pFBA) [40]. Fig. 2 displays that with  
 171 increasing light absorption, the rate of terpenoid synthesis in photosynthetic GTs increases up until approximately  $50$   
 172  $\frac{\mu\text{mol Photons}}{\text{s} \cdot \text{m}^2}$ . This increase in terpenoid synthesis rate with increasing absorbed light is particularly interesting due to  
 173 the fact that the model can not utilise atmospheric carbon dioxide, and sucrose is the only carbon source. This means  
 174 that there is a change in metabolic fluxes which enables this increase in terpenoid synthesis rate. To further investi-  
 175 gate what changes in the metabolism of photosynthetic GTs in increasing light intensities, we inspect the respective  
 176 changes in the exchange fluxes of the model. Fig. 2 shows the exchange fluxes of carbon dioxide and oxygen in our

177 pFBA model simulations over increasing light absorptions. Noticeably, the release of carbon dioxide systematically  
178 decreases up until approximately  $50 \frac{\mu\text{mol Photons}}{\text{s}\cdot\text{m}^2}$ . Interestingly, the consumption of oxygen decreases to zero at ap-  
179 proximately  $21 \frac{\mu\text{mol Photons}}{\text{s}\cdot\text{m}^2}$ . From this light intensity on, oxygen release begins and increases until  $50 \frac{\mu\text{mol Photons}}{\text{s}\cdot\text{m}^2}$ .  
180 These observations are crucial for a general understanding of the model behaviour. An increase in absorbed light  
181 causes higher photosynthetic activity, resulting in oxygen production. This explains the decreasing oxygen uptake  
182 and the switch to oxygen release at  $21 \frac{\mu\text{mol Photons}}{\text{s}\cdot\text{m}^2}$  absorbed light. However, the steady decrease in carbon dioxide  
183 excretion is especially noteworthy. Most carbon dioxide is produced within catabolism, therefore the model behaviour  
184 hints at a decrease in catabolic activity in higher light intensities.

185 To investigate how the catabolic activity in our model simulations changes over increasing light intensities, we  
186 further inspect representative reactions for relevant catabolic pathways in our model. As sucrose, a disaccharide is  
187 the only carbon source in our model, we inspect representatives of the upper glycolysis, the lower glycolysis and the  
188 TCA cycle. Fig. 3 displays the fluxes of these reactions over different light intensities (shown on the x-axis as fractions  
189 of saturating light intensities) relative to their fluxes in the dark. The sucrose synthase and saccharase represent upper  
190 glycolysis activity. The 6-phosphofruktokinase, GAP dehydrogenase, and pyruvate kinase represent lower glycolysis  
191 activity and the pyruvate dehydrogenase and the citrate synthase represent TCA cycle activity. Furthermore, the  
192 RuBisCO rate is displayed to monitor the rate of carbon refixation. The results show that fluxes of upper glycolysis  
193 remain completely unchanged in increasing light intensities, however, the fluxes in lower glycolysis decrease in higher  
194 light conditions. An even higher impact can be observed for the TCA cycle activity. The pyruvate dehydrogenase  
195 activity steadily decreases, and the citrate synthase activity abruptly decreases in increasing light conditions. These  
196 observations show that catabolic pathways which are not responsible for energy and redox equivalent production  
197 (like upper glycolysis) are unaffected by increasing light intensities. However, the lower glycolysis and the TCA cycle,  
198 both catabolic pathways that produce energy and redox equivalents, display a strong flux decrease in higher light  
199 conditions. There is no reason to think that trichomes would not have the same regulatory mechanisms as mesophyll  
200 cells, leading to decreased glycolysis in higher light conditions. Increased photosynthesis is accompanied by increased  
201 photorespiration, which eventually supplies reducing equivalents in the mitochondria, which can then be used to fuel  
202 the respiratory electron transport chain [41]. The increase in terpenoid synthesis flux observed in Fig. 2, and the  
203 decrease in catabolic fluxes in Fig. 3 strongly suggest that increasing light conditions **shift the carbon partitioning**  
204 **from catabolic to anabolic pathways**. This shift is enabled due to the energy and redox equivalent production of  
205 the photosynthetic electron transport chain in photosynthetic GTs. The metabolic network is not dependent on the  
206 energy from oxidising carbon bodies in high-light conditions, and can therefore use more of those carbon bodies  
207 in terpenoid synthesis pathways. Interestingly, RuBisCO activity increases in higher light intensities, displaying that  
208 only very high levels of photosynthetic energy supply allows the refixation of carbon that is lost as carbon dioxide in  
209 anabolic processes (like terpenoid synthesis). GAP, pyruvate and acetyl-CoA are carbon bodies which can be used to  
210 produce either energy and redox equivalents or terpenoid precursors. Acetyl-CoA is the initial substrate of the TCA  
211 cycle in which it is oxidised to gain energy and redox equivalents but is also the initial substrate of the MEV pathway,  
212 also known as the isoprenoid pathway, which is the primary terpenoid synthesis pathway in non-photosynthetic GTs.  
213 GAP and pyruvate are metabolites within the lower glycolysis pathway and also initial substrates of the MEP which  
214 is a terpenoid synthesis pathway present in photosynthetic GTs.

215 To further analyse how the consumption of these metabolites depends on the illumination, we simulated the  
216 relative consumption rate of GAP/pyruvate and Acetyl-CoA by the aforementioned pathways over increasing light  
217 intensities. Fig. 4 displays the proportions of the consumption of these compounds by the TCA, MEV and MEP  
218 pathways. In low light intensities, more than half of the substrates are consumed by the MEV pathway, and the  
219 remainder is consumed by the TCA cycle, in both cases in the form of acetyl-CoA. In higher light intensities, the

220 fraction of substrates consumed by the TCA cycle is decreasing until it does not consume any more substrates. At this  
221 point, the relative flux of lower glycolysis starts decreasing, and the MEP pathway is beginning to consume proportions  
222 of the substrates, gradually taking over. This is a very important observation that shows that increasing light intensities,  
223 leading to higher energy levels due to photosynthetic activity, shift the carbon partitioning from catabolic to anabolic  
224 pathways by reducing the TCA cycle and lower glycolytic flux and increasing terpenoid synthesis. Furthermore, it  
225 shows that the two terpenoid synthesis pathways, MEP and MEV, are more advantageous at different energetic levels.  
226 In lower light intensities, and therefore lower energetic levels, the MEV pathway seems to be more advantageous  
227 because the conversion of GAP and pyruvate to acetyl-CoA produces energy and redox equivalents, and the resulting  
228 acetyl-CoA can directly be used in the TCA cycle to generate additional energy and redox equivalents. In higher  
229 light intensities, and therefore higher energetic levels, the MEP pathway is more advantageous because the high  
230 energy levels provided by photosynthetic activity remove the necessity of providing energy and redox equivalents  
231 via lower glycolysis and the TCA cycle. Instead, GAP and pyruvate can directly be used as substrates with higher  
232 energy contents (than acetyl-CoA) in the MEP pathway, and therefore further increase the fraction of carbon used in  
233 anabolism, enabling more efficient terpenoid synthesis.

234 This phenomenon can also be observed in Fig. 6, in which we used model simulations to calculate the fluxes  
235 of the final MEV and MEP reactions in systematically changing light conditions and ATP maintenance costs. In this  
236 analysis, higher ATP maintenance costs reflect increased energy requirements of cells in e.g. stress conditions. At low  
237 light conditions and low ATP maintenance costs, the MEV pathway is the main terpenoid synthesis pathway, with  
238 very little MEP pathway activity. In low light conditions and high ATP maintenance costs, the MEV pathway is the  
239 only active pathway. However, the overall terpenoid synthesis flux is relatively low due to the increased demand  
240 for catabolic flux in such conditions. At high light conditions and high ATP maintenance costs, the MEP pathway is  
241 carrying the majority of terpenoid synthesis flux. In high light conditions and low ATP maintenance costs, the MEP  
242 pathway is the only active terpenoid synthesis pathway, providing the highest terpenoid synthesis flux. It appears  
243 that the distribution of terpenoid synthesis between the MEV and the MEP pathways is highly dependent on the light  
244 conditions and resulting energy levels of the photosynthetic GTs.

245 The general conclusions of our model simulations have then been tested experimentally. The impact of light  
246 intensity on the shift from the MEV to MEP precursor pathway has been tested by quantifying sesquiterpenes, pro-  
247 duced by MEV, and monoterpenes, produced by MEP. Three-week-old tomato (*Solanum lycopersicum* cv MoneyMaker)  
248 plants were exposed to nearly threefold higher light intensity (HL) for seven days and the productivity of the main  
249 volatile terpenoids produced in the type VI GTs was estimated by GC-MS along different leaf developmental stages.  
250 The results showed a significant increase in monoterpenoids while the sesquiterpenes remained unchanged and such  
251 increment is linked to the age of the leaves (Fig. 5). These findings suggest that the photosynthetic light reactions  
252 support the productivity of the specialised reactions occurring in the plastids through the MEP pathway.

253 Finally, the high rate of terpenoid synthesis in high-light conditions is partly resulting from increased rates of  
254 carbon refixation. It remains unknown how active the CBB cycle is in photosynthetic GTs. To quantify the impact of  
255 different carbon refixation fluxes, we performed a systematic analysis in which we calculated the terpenoid synthesis  
256 rate over different quanta of **absorbed light** and systematically changed the activities of RuBisCO (Fig. 7). Interestingly,  
257 the overall rate of carbon refixation is increasing the rate of terpenoid synthesis by almost 20%, while the shift in  
258 carbon partitioning between catabolism and anabolism increases it by almost 200%. This shows that the impact of  
259 energy-dependent shift in carbon partitioning and isoprenoid synthesis pathways is a lot higher than the RuBisCO-  
260 dependent refixation of carbon dioxide.



## 261 4 | DISCUSSION

262 In photosynthetic GTs, synthetic pathways of terpenoids and other secondary metabolites are found in the cytosol of  
263 the cells and the chloroplasts. The additional terpenoid synthesis pathway in photosynthetic GTs has been subject to  
264 many speculations, e.g., terpenoid production in chloroplasts is specialised for the production of particular secondary  
265 metabolites [28]. In our work, we built a simplified, yet data-driven constraint-based model of photosynthetic glandular  
266 trichome metabolism, and used it to show that one of the two different synthesis pathways is more advantageous  
267 for terpenoid production than the other in different energy availabilities. Previously published multi-omics data [5]  
268 supports our hypothesis that the energy and reducing power (ATP and NADPH) from photosynthesis are primarily  
269 used to power the secondary metabolism. Our model provides a mechanistic explanation of how this is achieved.

270 We show that with lower energy availability, the cytosolic MEV pathway is more advantageous for terpenoid  
271 synthesis because the catabolic pathways, producing the critical initial substrate acetyl-CoA from sucrose, provide  
272 additional energy and redox equivalents needed for all cellular activities, including terpenoid synthesis. However,  
273 higher energy availability (coming from photosynthetic activity in higher light conditions) removes the need for the  
274 additional energy and redox equivalents gained from the conversion of sucrose to acetyl-CoA. Therefore substrates  
275 with higher energy levels (GAP and pyruvate) can be directly used for terpenoid synthesis. This shortcut of catabolic  
276 reactions reduces the loss of carbon as carbon dioxide and increases the flux of carbon through anabolic processes.  
277 The general conclusions derived from the theoretical analyses have been strengthened with the experimental evidence  
278 that under higher light intensities production of monoterpenoids is significantly increased, whilst the production of  
279 sesquiterpenes remains unchanged (Fig. 5).

280 We show that in higher light conditions, energy levels of the photosynthetic GTs are so advantageous, that excess  
281 energy can be spent to perform carbon refixation using the CBB cycle. In the supplementary material, we calculated  
282 that the terpenoid yield per sucrose is twice as high in high light compared to low light conditions. This illustrates that  
283 the benefit of including chloroplasts in GTs is not only the ability to shift carbon partitioning from catabolic to anabolic  
284 processes but also to further maximize carbon use efficiency. It is important to note that the increase in terpenoid  
285 synthesis from carbon refixation is not nearly as high as the increase from the shift in carbon partitioning, as seen in  
286 Fig. 7. This dual behaviour, i.e. in the absence versus in presence of photosynthesis, is reminiscent of the situation in  
287 photosynthetic leaves, where the TCA cycle is inactive during the day and active during the night [42].

288 Interestingly our model shows that even without CBB cycle activity, the TCA cycle may be reversed in high energy  
289 availability and function as a reductive TCA cycle. This reductive TCA cycle could theoretically take over the function  
290 of the CBB cycle, using energy to fix carbon dioxide which was produced in catabolic and anabolic reactions, thus  
291 increasing carbon use efficiency. This is a very interesting observation, as, from a bioenergetic point of view, such  
292 a scenario is possible. Considering the previous results where Phosphoenolpyruvate carboxylase (PEPC) expression  
293 was significantly increased in trichomes compared to leaves [5], we consider PEPC as a plausible candidate to mediate  
294 the carbon fixation. However, we decided to adjust the key reactions of the TCA cycle for this scenario as irreversible  
295 to prevent this phenomenon to be included in our results for now. The reason for this decision is that the reductive  
296 TCA cycle is usually found in green sulfur bacteria and different thermophilic prokaryotes and archaea [43, 44]. This  
297 indicates that from a phylogenetic perspective, the presence of a reductive TCA cycle in photosynthetic GTs is rather  
298 unlikely. However, we think that this model suggestion is worth investigating the fluxes of the TCA cycle in light  
299 conditions in photosynthetic GTs, as it has been suggested that carbon dioxide may be recovered [45]. Generally, instead  
300 of showing that chloroplastic terpenoid synthesis pathways provide improved production of particular terpenoids,  
301 our work shows that the chloroplast in photosynthetic GTs functions as a solar panel in light conditions, which can  
302 be used to shift carbon from catabolic to anabolic fluxes and even enable carbon dioxide refixation and therefore

303 improve carbon use efficiency. To support our findings, experiments are needed which can keep track of the rate of  
304 terpenoid synthesis in similar sucrose availability but different light absorptions. Interestingly, such an increase in the  
305 efficiency of carbon use through RubisCO, but without the CBB cycle, has been observed in other plant cells. Schwen-  
306 der *et al.* [46] showed that Rubisco without the Calvin cycle improves the carbon efficiency of developing embryos of  
307 *Brassica napus L.* (oilseed rape) during the formation of oil.

308 Photosynthetic carbon refixation indicates that photorespiration may be present in photosynthetic GTs. Although  
309 photorespiratory genes were very low expressed in the transcriptome data [5], and photorespiration is not included in  
310 our model, we show that in high light there is oxygen evolution in photosynthetic GTs. Therefore, new experimental  
311 data obtained in high light intensities and gas exchange rates is required to investigate putative photorespiratory ac-  
312 tivities. Furthermore, it remains unclear if and how high the evolution of reactive oxygen species and photodamage is  
313 present in photosynthetic GTs. For this, quantitative metabolic data for the components of the electron transport chain  
314 is needed, as well as measurements of the photosynthetic efficiency in photosynthetic GTs. Finally, more questions  
315 regarding the dynamics, and not only bioenergetics of trichomes arise. E.g., what is the composition of terpenoids  
316 under different light intensities, or even light colours? A recent study using different basil cultivars showed that light  
317 spectra affect the concentrations and volatile emissions of important compounds [47]. Such light modulation requires  
318 further investigation with a use of more detailed models of secondary metabolism in photosynthetic GTs that take  
319 the light spectrum into consideration. For transparency, we include the light spectra used for our experimental vali-  
320 dation in Fig. S1. As most of the processes discussed here are heavily dependent on enzyme kinetics and saturation,  
321 constraint-based models like the one presented may not be the best method for answering these new emerging ques-  
322 tions. Mechanistic models, e.g. based on ordinary differential equations, can include such information (if available) and  
323 may be helpful to give further insights into terpenoid synthesis in photosynthetic GTs. Further interdisciplinary stud-  
324 ies combining experiments and robust theoretical simulations can provide a quantitative understanding of whether,  
325 how, and by how much the production of specific terpenoids could be increased, and with this work, we provide the  
326 stepping stone for such analyses. The outcomes of this research provide quantitative measures to assess the bene-  
327 ficial role of chloroplast in GTs and can further guide the design of new experiments aiming at enhanced terpenoid  
328 production.

## 329 Acknowledgements

## 330 Conflict of interest

331 The authors declare that they have no conflict of interest.

## 332 Supporting Information

333 The computational model presented here, together with the Jupyter Notebook containing step-by-step instructions  
334 on how to reconstruct the model and reproduce all analyses included in this manuscript are openly available on the  
335 GitLab repository <https://gitlab.com/qtb-hhu/models/glandular-trichomes> or can be requested from the au-  
336 thors.

## references

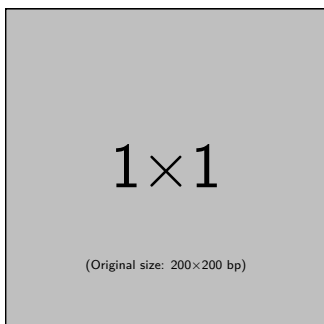
- [1] E Werker. Trichome diversity and development. *Adv. Bot. Res.*, 31:1–35, jan 2000. ISSN 0065-2296. doi: 10.1016/S0065-2296(00)31005-9.

- [2] Jon F. Fobes, J. Brian Mudd, and Margery P. F. Marsden. Epicuticular Lipid Accumulation on the Leaves of *Lycopersicon pennellii* (Corr.) D'Arcy and *Lycopersicon esculentum* Mill. *Plant Physiology*, 77(3):567–570, 03 1985. ISSN 0032-0889. doi: 10.1104/pp.77.3.567. URL <https://doi.org/10.1104/pp.77.3.567>.
- [3] Alexandre Huchelmann, Marc Boutry, and Charles Hachez. Plant Glandular Trichomes: Natural Cell Factories of High Biotechnological Interest. *Plant Physiol.*, 175(September):6–22, 2017. doi: 10.1104/pp.17.00727.
- [4] Joris J. Glas, Bernardus C.J. Schimmel, Juan M. Alba, Rocío Escobar-Bravo, Robert C. Schuurink, and Merijn R. Kant. Plant glandular trichomes as targets for breeding or engineering of resistance to herbivores. *International Journal of Molecular Sciences*, 13(12):17077–17103, 2012. ISSN 14220067. doi: 10.3390/ijms131217077.
- [5] Gerd U. Balcke, Stefan Bennewitz, Nick Bergau, Benedikt Athmer, Anja Henning, Petra Majovsky, José M. Jiménez-Gómez, Wolfgang Hoehenwarter, and Alain Tissier. Multi-Omics of Tomato Glandular Trichomes Reveals Distinct Features of Central Carbon Metabolism Supporting High Productivity of Specialized Metabolites. *The Plant Cell*, 29(5): 960–983, 04 2017. ISSN 1040-4651. doi: 10.1105/tpc.17.00060.
- [6] R. W.J. Kortbeek, J. Xu, A. Ramirez, E. Spyropoulou, P. Diergaarde, I. Otten-Bruggeman, M. de Both, R. Nagel, A. Schmidt, R. C. Schuurink, and P. M. Bleeker. Engineering of Tomato Glandular Trichomes for the Production of Specialized Metabolites. *Methods in Enzymology*, 576:305–331, 2016. ISSN 15577988. doi: 10.1016/bs.mie.2016.02.014.
- [7] Heike Paetzolda, Stefan Garms, Stefan Bartramb, Jenny Wieczorek, Eva-Maria Uros-Gracia, Manuel Rodriguez-Concepcion, Wilhelm Boland, Dieter Strack, Bettina Hause, and Michael H. Walter. The Isogene 1-Deoxy-D-Xylulose 5-Phosphate Synthase 2 Controls Isoprenoid Profiles, Precursor Pathway Allocation, and Density of Tomato Trichomes. *Mol. Plant*, 3(5):904–916, 2010. doi: 10.1093/mp/ssq032.
- [8] Somnath Koley, Eva Grafahrend-Belau, Manish L. Raorane, and Björn H. Junker. The mevalonate pathway contributes to monoterpene production in peppermint. *bioRxiv*, 2020. doi: 10.1101/2020.05.29.124016.
- [9] Nick Bergau, Stefan Bennewitz, Frank Syrowatka, Gerd Hause, and Tissier, A. The development of type VI glandular trichomes in the cultivated tomato *Solanum lycopersicum* and a related wild species *S. habrochaites*. *BMC Plant Biol.*, 15(289):1–15, 2015. ISSN 1471-2229. doi: 10.1186/s12870-015-0678-z.
- [10] Sari A. Ruuska, Jorg Schwender, and John B. Ohlrogge. The Capacity of Green Oilseeds to Utilize Photosynthesis to Drive Biosynthetic Processes. *Plant Physiology*, 136(1):2700–2709, 09 2004. doi: 10.1104/pp.104.047977.
- [11] Fernando D. Goffman, Ana P. Alonso, Jorg Schwender, Yair Shachar-Hill, and John B. Ohlrogge. Light Enables a Very High Efficiency of Carbon Storage in Developing Embryos of Rapeseed. *Plant Physiology*, 138(4):2269–2279, 07 2005. ISSN 0032-0889. doi: 10.1104/pp.105.063628.
- [12] Rocío Escobar-Bravo, Jasmijn Ruijgrok, Hye Kyong Kim, Katharina Grosser, Nicole M Van Dam, Peter G L Klinkhamer, and Kirsten A Leiss. Light intensity-mediated induction of trichome-associated allelochemicals increases resistance against thrips in tomato. *Plant cell physiology*, 59(12):2462–2475, 2018. doi: 10.1093/pcp/pcy166.
- [13] Alejandro Brand and Alain Tissier. Control of resource allocation between primary and specialized metabolism in glandular trichomes. *Current Opinion in Plant Biology*, 66:102172, 2022. ISSN 1369-5266. doi: 10.1016/j.pbi.2022.102172.
- [14] Timo R. Maarleveld, Ruchir A. Khandelwal, Brett G. Olivier, Bas Teusink, and Frank J. Bruggeman. Basic concepts and principles of stoichiometric modeling of metabolic networks. *Biotechnol. J.*, 8(9):997–1008, 2013. ISSN 18606768. doi: 10.1002/biot.201200291.
- [15] Reinhart Heinrich and Stefan Schuster. The regulation of cellular systems. *Book*, page 416, 1996. doi: 10.1007/978-1-4613-1161-4.
- [16] Ankita Chatterjee, Benazir Huma, Rahul Shaw, and Sudip Kundu. Reconstruction of *Oryza sativa indica* Genome Scale Metabolic Model and Its Responses to Varying RuBisCO Activity, Light Intensity, and Enzymatic Cost Conditions. *Front. Plant Sci.*, 8(November):1–18, 2017. ISSN 1664-462X. doi: 10.3389/fpls.2017.02060.

- [17] Mark G Poolman, Laurent Miguet, Lee J Sweetlove, and David A Fell. A Genome-scale Metabolic Model of *Arabidopsis thaliana* and Some of its Properties. *Plant Physiol.*, 151(November):1570–1581, 2009. ISSN 0032-0889. doi: 10.1104/pp.109.141267.
- [18] Huili Yuan, C.Y. Maurice Cheung, Mark G. Poolman, Peter A. J. Hilbers, and Natal A. W. van Riel. A genome-scale metabolic network reconstruction of tomato (*Solanum lycopersicum* L.) and its application to photorespiratory metabolism. *Plant J.*, 85(2):289–304, 2016. ISSN 09607412. doi: 10.1111/tpj.13075.
- [19] Jeffrey D Orth, Ines Thiele, and Bernhard Ø Palsson. What is flux balance analysis? *Nat. Biotechnol.*, 28(3):245–248, 2011. doi: 10.1038/nbt.1614.What.
- [20] L J Sweetlove and R G Ratcliffe. Flux-balance modeling of plant metabolism. *Front Plant Sci*, 2:38, 2011.
- [21] The Tomato Genome Consortium. The tomato genome sequence provides insights into fleshy fruit evolution. *Nature*, 485:635–641, 2012. doi: doi.org/10.1038/nature11119.
- [22] Vasiliki Falara, Tariq A. Akhtar, Thuong T.H. Nguyen, Eleni A. Spyropoulou, Petra M. Bleeker, Ines Schauvinhold, Yuki Matsuba, Megan E. Bonini, Anthony L. Schillmiller, Robert L. Last, Robert C. Schuurink, and Eran Pichersky. The tomato terpene synthase gene family. *Plant Physiology*, 157(2):770–789, 2011. ISSN 15322548. doi: 10.1104/pp.111.179648.
- [23] Rigoberto Rios-Esteva, Glenn W Turner, James M Lee, Rodney B Croteau, and B Markus Lange. A systems biology approach identifies the biochemical mechanisms regulating monoterpene essential oil composition in peppermint. *Proc. Natl. Acad. Sci. USA*, 105(8):2818–2823, 2008.
- [24] Rigoberto Rios-Esteva, Iris Lange, James M Lee, and B Markus Lange. Mathematical Modeling-Guided Evaluation of Biochemical, Developmental, Environmental, and Genotypic Determinants of Essential Oil Composition and Yield in Peppermint Leaves. *Plant Physiol.*, 152:2105–2119, 2010. doi: 10.1104/pp.109.152256.
- [25] Nima P. Saadat, Marvin van Aalst, and Oliver Ebenhöf. Network reconstruction and modelling made reproducible with moped. *Metabolites*, 12(4), 2022. ISSN 2218-1989. doi: 10.3390/metabo12040275.
- [26] N. Fernandez-Pozo, N. Menda, JD. Edwards, S. Saha, IY Tecle, SR Strickler, A Bombarely, T Fisher-York, A Pujar, H Forster, A Yan, and LA Mueller. The sol genomics network (sgn) from genotype to phenotype to breeding. *Nucleic Acids Res.*, 43 (Database issue):D1036–41, 2015.
- [27] Sylvain Prigent, Clémence Frioux, Simon M Dittami, Sven Thiele, Abdelhalim Larhlmi, Guillaume Collet, Fabien Gutknecht, Jeanne Got, Damien Eveillard, Jérémie Bourdon, et al. Meneco, a topology-based gap-filling tool applicable to degraded genome-wide metabolic networks. *PLoS computational biology*, 13(1):e1005276, 2017.
- [28] Katrin Besser, Andrea Harper, Nicholas Welsby, Ines Schauvinhold, Stephen Slocombe, Yi Li, Richard A Dixon, and Pierre Broun. Divergent regulation of terpenoid metabolism in the trichomes of wild and cultivated tomato species. *Plant physiology*, 149(1):499–514, 2009.
- [29] Per Gardeström and Abir U Igamberdiev. The origin of cytosolic atp in photosynthetic cells. *Physiologia Plantarum*, 157(3):367–379, 2016.
- [30] Christian Lieven, Moritz E Beber, Brett G Olivier, Frank T Bergmann, Meric Ataman, Parizad Babaei, Jennifer A Bartell, Lars M Blank, Siddharth Chauhan, Kevin Correia, et al. Memote for standardized genome-scale metabolic model testing. *Nature biotechnology*, 38(3):272–276, 2020.
- [31] Willi Gottstein, Brett G. Olivier, Frank J. Bruggeman, and Bas Teusink. Constraint-based stoichiometric modelling from single organisms to microbial communities. *Journal of The Royal Society Interface*, 13(124):20160627, 2016. doi: 10.1098/rsif.2016.0627.
- [32] Samuel MD Seaver, Louis MT Bradbury, Océane Frelin, Raphy Zarecki, Eytan Ruppim, Andrew D Hanson, and Christopher S Henry. Improved evidence-based genome-scale metabolic models for maize leaf, embryo, and endosperm. *Frontiers in plant science*, 6:142, 2015.

- [33] A. Arnold and Z. Nikoloski. Bottom-up Metabolic Reconstruction of Arabidopsis and Its Application to Determining the Metabolic Costs of Enzyme Production. *Plant Physiol.*, 165(3):1380–1391, 2014. ISSN 0032-0889. doi: 10.1104/pp.114.235358.
- [34] Jordan J. Zager and B. Markus Lange. Assessing Flux Distribution Associated with Metabolic Specialization of Glandular Trichomes. *Trends in Plant Science*, 23(7):638–647, 2018. ISSN 13601385. doi: 10.1016/j.tplants.2018.04.003.
- [35] CY Maurice Cheung, Thomas CR Williams, Mark G Poolman, David A Fell, R George Ratcliffe, and Lee J Sweetlove. A method for accounting for maintenance costs in flux balance analysis improves the prediction of plant cell metabolic phenotypes under stress conditions. *The plant journal*, 75(6):1050–1061, 2013.
- [36] Lee James Conneely, Ramil Mauleon, Jos Mieog, Bronwyn J. Barkla, and Tobias Kretzschmar. Characterization of the cannabis sativa glandular trichome proteome. *PLOS ONE*, 16(4):1–26, 04 2021. doi: 10.1371/journal.pone.0242633. URL <https://doi.org/10.1371/journal.pone.0242633>.
- [37] C.Y. Maurice Cheung, Mark G. Poolman, David. A. Fell, R. George Ratcliffe, and Lee J. Sweetlove. A Diel Flux Balance Model Captures Interactions between Light and Dark Metabolism during Day-Night Cycles in C3 and Crassulacean Acid Metabolism Leaves. *Plant Physiology*, 165(2):917–929, 03 2014. ISSN 0032-0889. doi: 10.1104/pp.113.234468.
- [38] Glenn W Turner and Rodney Croteau. Organization of monoterpene biosynthesis in mentha. immunocytochemical localizations of geranyl diphosphate synthase, limonene-6-hydroxylase, isopiperitenol dehydrogenase, and pulegone reductase. *Plant physiology*, 136(4):4215–4227, 2004.
- [39] Radosław Kowalski, Grażyna Kowalska, Monika Jankowska, Agnieszka Nawrocka, Klaudia Kałwa, Urszula Pankiewicz, and Marzena Włodarczyk-Stasiak. Secretory structures and essential oil composition of selected industrial species of lamiaceae. *Acta Scientiarum Polonorum Hortorum Cultus*, 8:2, 2019.
- [40] Nathan E Lewis, Kim K Hixson, Tom M Conrad, Joshua A Lerman, Pep Charusanti, Ashoka D Polpitiya, Joshua N Adkins, Gunnar Schramm, Samuel O Purvine, Daniel Lopez-Ferrer, Karl K Weitz, Roland Eils, Rainer König, Richard D Smith, and Bernhard Ø Palsson. Omic data from evolved e. coli are consistent with computed optimal growth from genome-scale models. *Molecular Systems Biology*, 6(1):390, 2010. doi: 10.1038/msb.2010.47.
- [41] Gerd Ulrich Balcke, Khabat Vahabi, Jonas Giese, Iris Finkemeier, and Alain Tissier. The arabidopsis concert of metabolic acclimation to high light stress. *bioRxiv*, 2023. doi: 10.1101/2023.02.14.528433. URL <https://www.biorxiv.org/content/early/2023/02/15/2023.02.14.528433>.
- [42] Guillaume Tcherkez and Owen K. Atkin. Unravelling mechanisms and impacts of day respiration in plant leaves: an introduction to a virtual issue. *New Phytologist*, 230(1):5–10, 2021. doi: 10.1111/nph.17164.
- [43] Thomas M Wahlund and F Robert Tabita. The reductive tricarboxylic acid cycle of carbon dioxide assimilation: initial studies and purification of atp-citrate lyase from the green sulfur bacterium chlorobium tepidum. *Journal of bacteriology*, 179(15):4859–4867, 1997.
- [44] Monika Beh, Gerhard Strauss, Robert Huber, Karl-Otto Stetter, and Georg Fuchs. Enzymes of the reductive citric acid cycle in the autotrophic eubacterium aquifex pyrophilus and in the archaeobacterium thermoproteus neutrophilus. *Archives of Microbiology*, 160(4):306–311, 1993.
- [45] Robert Schuurink and Alain Tissier. Glandular trichomes: micro-organs with model status? *New Phytologist*, 225(6):2251–2266, 2020.
- [46] Jörg Schwender, Fernando D. Goffman, John B. Ohlrogge, and Yair Shachar-Hill. Rubisco without the calvin cycle improves the carbon efficiency of developing green seeds. *Nature*, 432:779–782, 2004.
- [47] Minna Kivimäenpää, Adedayo Mofikoya, Ahmed M. Abd El-Raheem, Johanna Riikonen, Riitta Julkunen-Tiitto, and Jarmo K. Holopainen. Alteration in light spectra causes opposite responses in volatile phenylpropanoids and terpenoids compared with phenolic acids in sweet basil (*ocimum basilicum*) leaves. *Journal of Agricultural and Food Chemistry*, 70(39):12287–12296, 2022. doi: 10.1021/acs.jafc.2c03309.

## GRAPHICAL ABSTRACT



Please check the journal's author guidelines for whether a graphical abstract, key points, new findings, or other items are required for display in the Table of Contents.

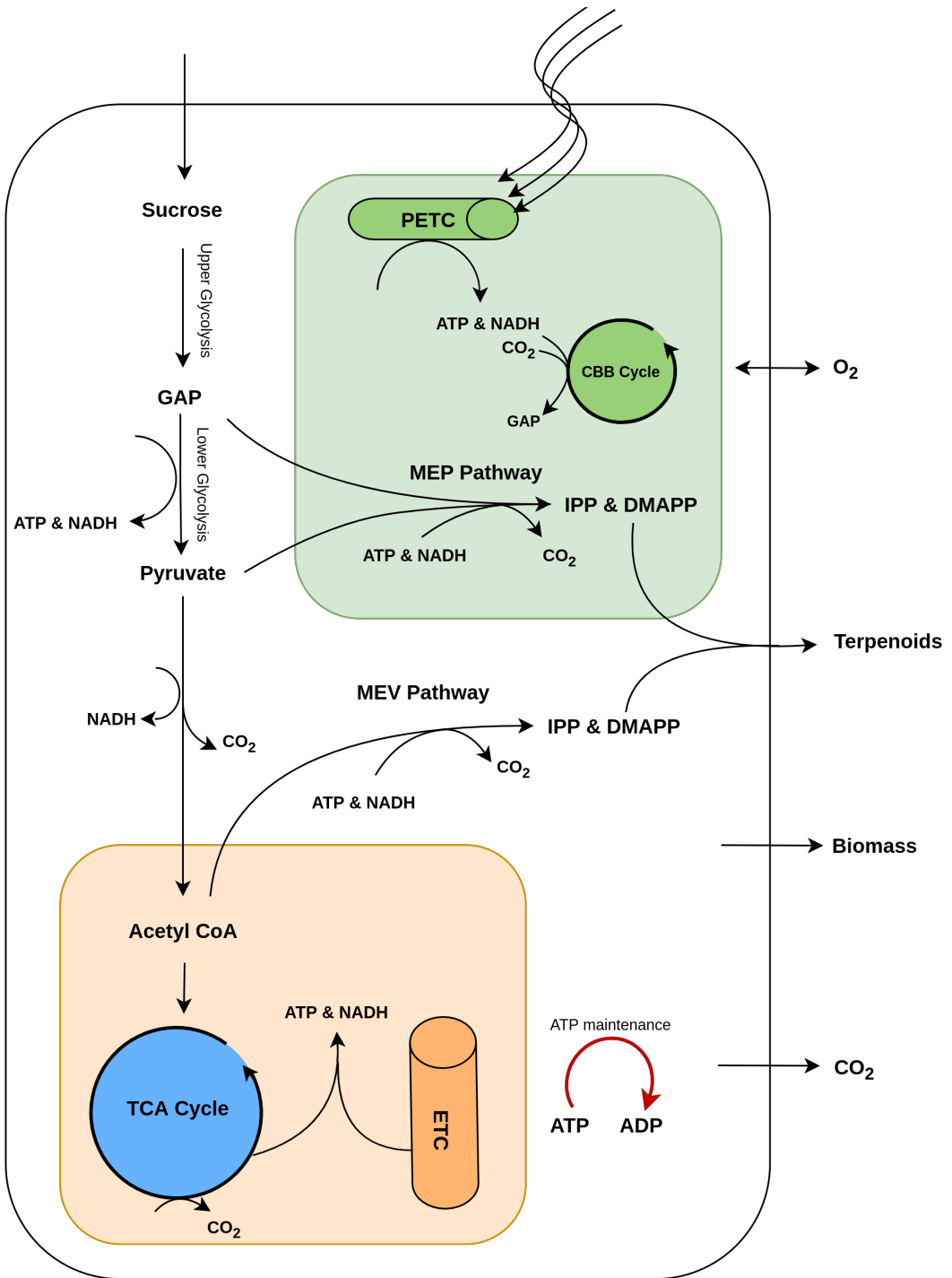


**FIGURE 1** Schematic overview of the key processes included in a constraint-based model of photosynthetic glandular trichome (GT) metabolism. While the model is built using transcriptome and metabolome data and includes a large number of reactions, only pathways and metabolites of importance to the results are highlighted in the presented model scheme. These include CBB Cycle, Calvin-Benson-Bassham Cycle; DMAPP, dimethylallyl diphosphate; IPP, isopentenyl diphosphate; MEP, methyl-erythritol phosphate pathway; MEV, mevalonate pathway; PETC, photosynthetic electron transfer chain; TCA Cycle, tricarboxylic acid Cycle.

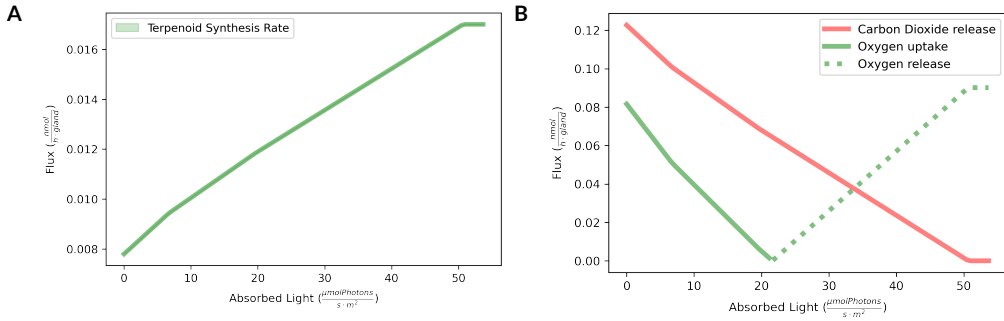


**FIGURE 2** Impact of rates of absorbed light on the predicted fluxes through the photosynthetic glandular trichome. **a** Terpenoid synthesis flux over different rates of absorbed light. The rate terpenoid synthesis increases with higher amounts of absorbed light. **b** Oxygen and carbon dioxide exchange fluxes over different rates of absorbed light. Increased light absorption decreases carbon dioxide release and oxygen absorption. In higher rates of light absorption, oxygen is secreted.

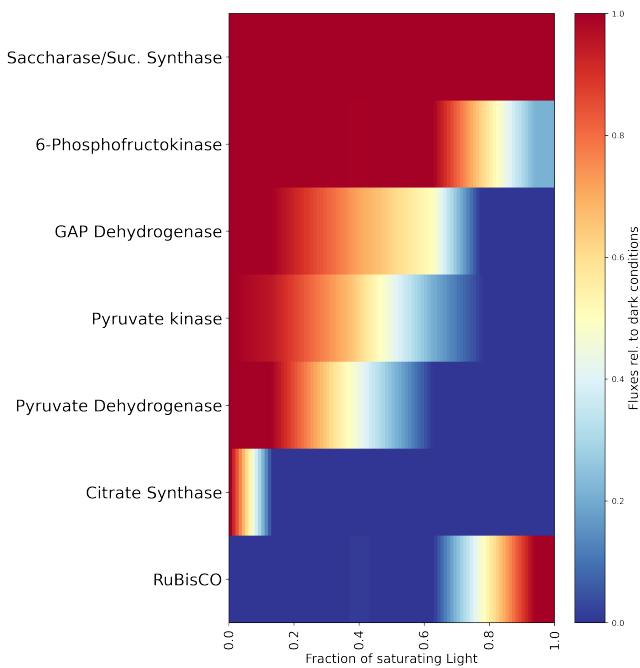


**FIGURE 3** The relative fluxes of six selected catabolic reactions and one carbon fixation reaction calculated for increasing fractions of saturating light. The fluxes are normalised to the respective fluxes under completely dark conditions. Reactions of upper glycolysis remain unaffected by increased light absorption, while the fluxes of reactions of lower glycolysis and the TCA cycle decrease with increased absorbed light. Additionally, RuBisCO flux is only present when light absorption is high.



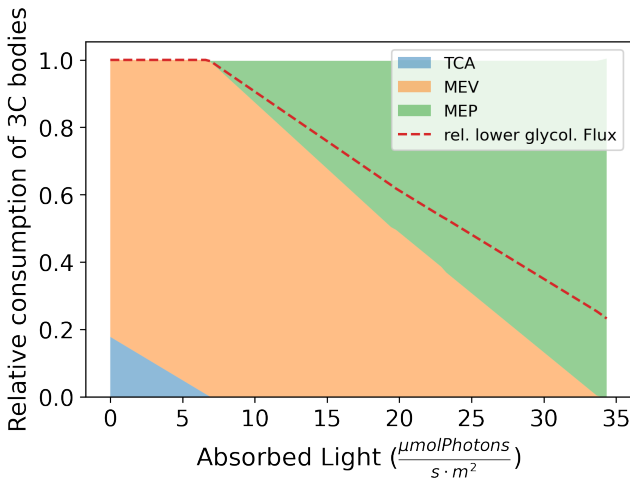
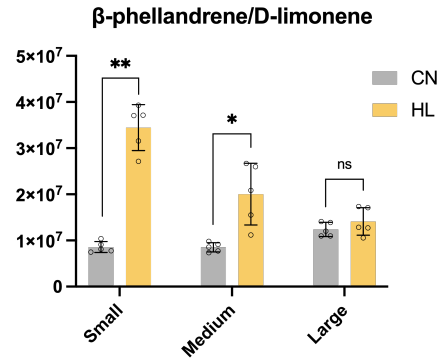
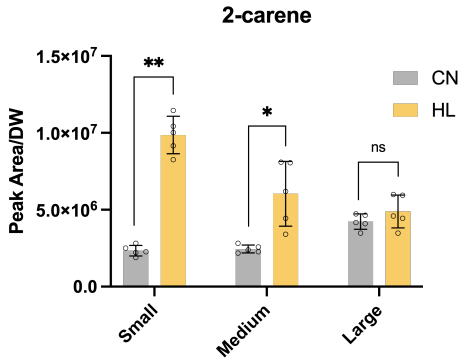


**FIGURE 4** Predicted relative consumption of GAP, pyruvate and acetyl-CoA (here described as 3C bodies) by different pathways over increasing fractions of saturating light. The fraction of the lower glycolysis flux relative to dark conditions is displayed as a dashed line. Increasing rates of absorbed light decrease the fraction of 3C bodies consumed by catabolic pathways, like lower glycolysis and TCA cycle. Furthermore, the fraction of 3C bodies consumed for terpenoid synthesis switches from the MEV to MEP pathway in high rates of light absorption.

### a. Monoterpenes



### b. Sesquiterpenes

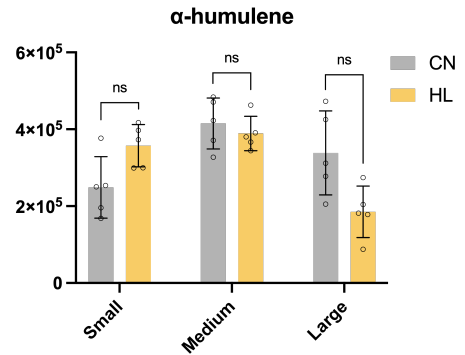
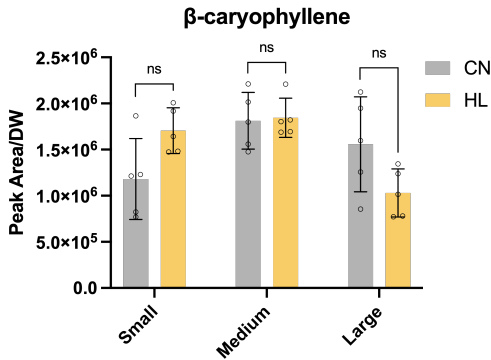


**FIGURE 5** Effect of high light in volatile terpene content of leaves of tomato. Estimation of (a) monoterpenes and (b) sesquiterpenes by gas chromatography-mass spectrometry (GC-MS) on young (Small, from bottom-to-top leaf number 6), expanded (Medium, leaf number 5) and fully develop (Large, leaf number 4) leaves, in control (CN) and high light (HL) conditions. Chromatogram peak areas were normalized by leaf dry weight (DW). Error bars indicate SD ( $n = 5$  biological replicates; \* $P < 0,05$ , \*\* $P < 0,01$ ; using  $t$ -test).

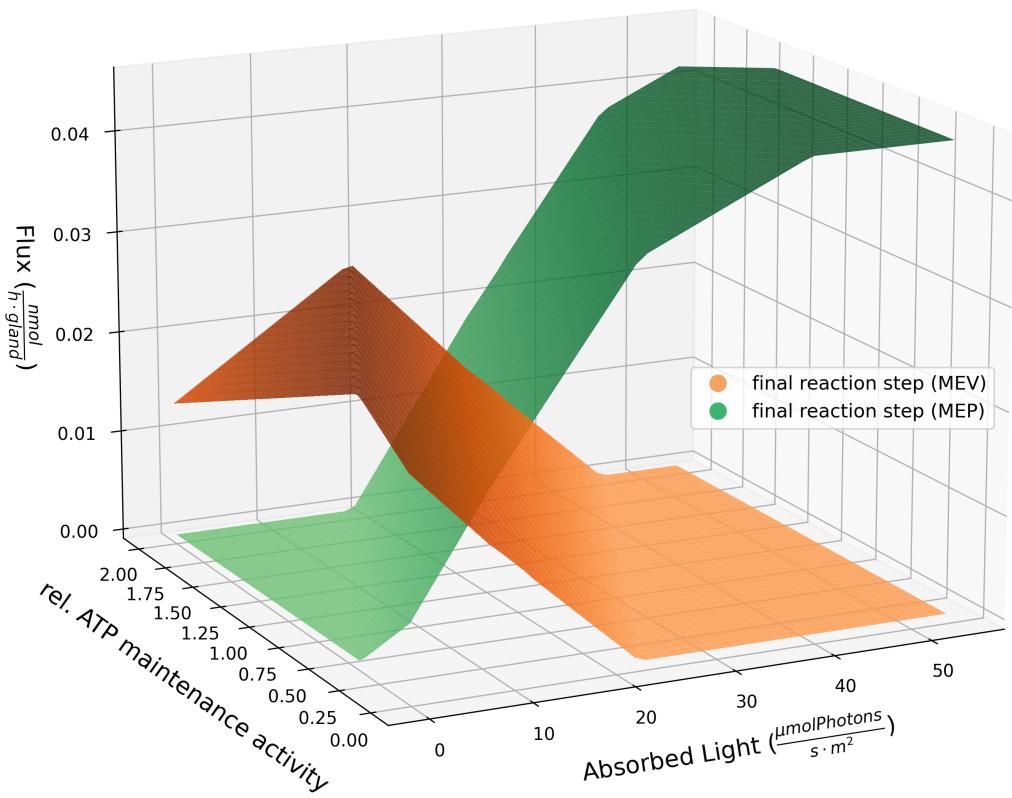


**FIGURE 6** Fluxes of the final reaction steps of the MEV and MEP pathway over increasing relative ATP maintenance activities, as well as increasing rates of light absorption. In energetically favorable conditions, like high light and low ATP maintenance (function representing the additional energy requirement for the maintenance of cells), terpenoid synthesis is carried out by the MEP pathway. In opposite conditions, meaning low light and high ATP maintenance, the MEV pathway is performing terpenoid synthesis.

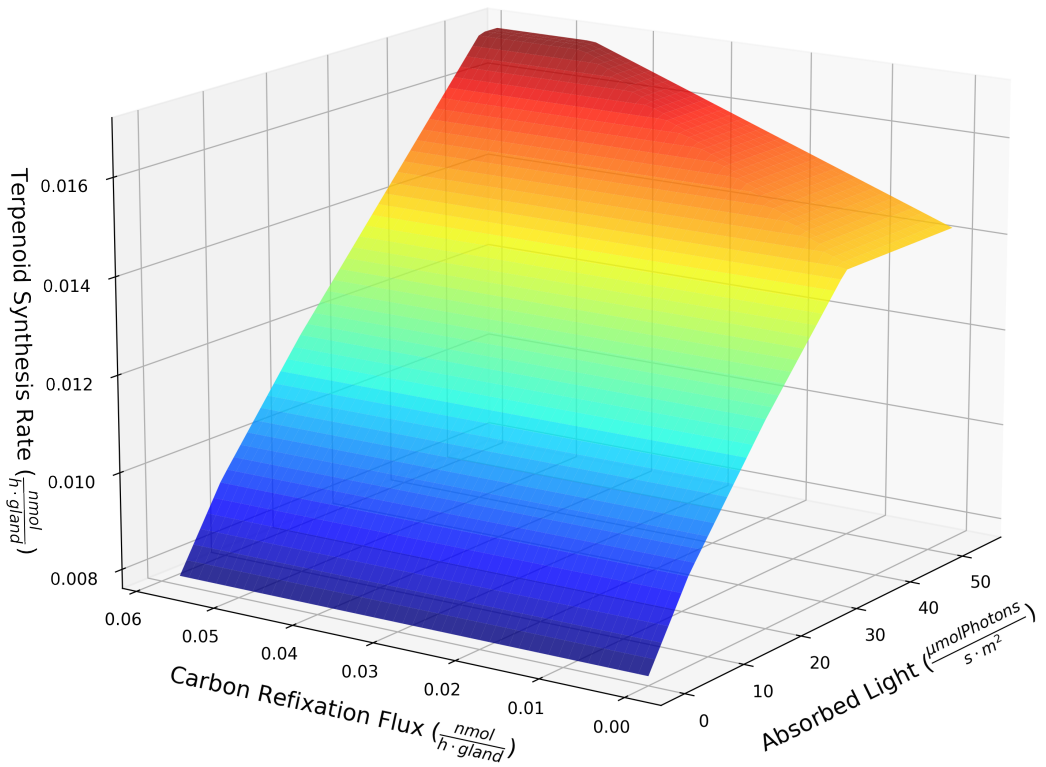


**FIGURE 7** Predicted flux of the terpenoid synthesis under changing carbon refixation rates, as well as increasing rates of light absorption. Under simulated saturating light, the rate of terpenoid synthesis is two-fold higher than in darkness. If additionally the carbon refixation flux is increased to the maximal chosen value, the increase in terpenoid synthesis is less than 20%. This result shows how the energy-dependent shift in carbon partitioning and isoprenoid synthesis pathway is higher than the RuBisCO dependent refixation of carbon dioxide.

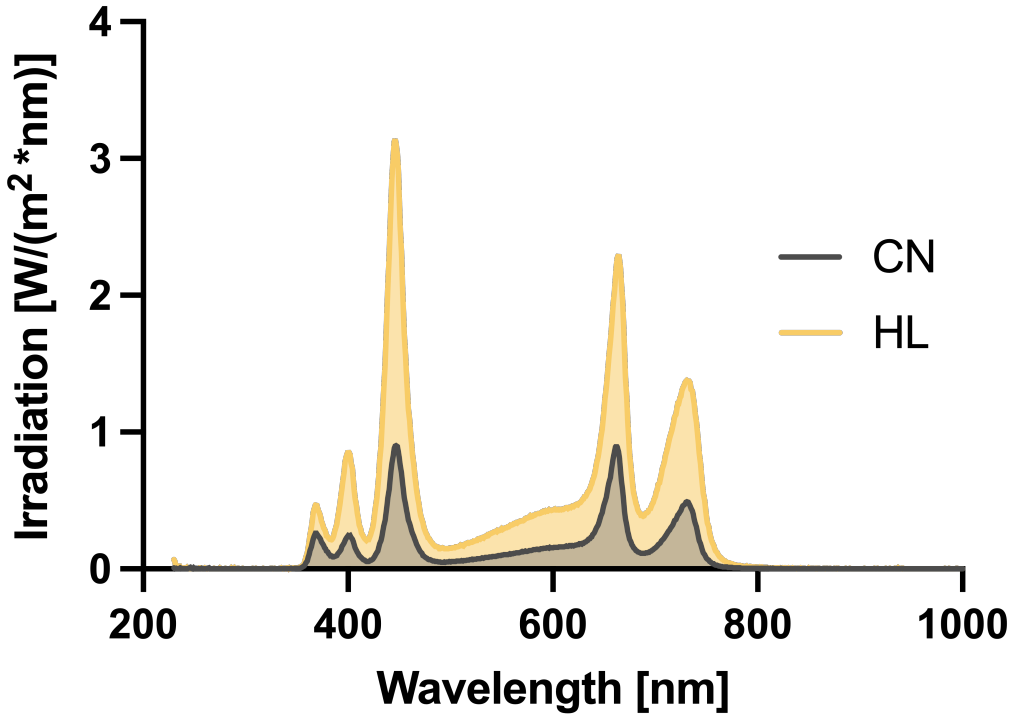


**FIGURE S1** Light spectra of the two light conditions used in the experiment. Wavelength recorded from 230 to 1000 nm. CN, control; HL, high light.